IMPROVEMENT OF THE NUMERICS AND DEEP-WATER PHYSICS IN AN ACADEMIC VERSION OF SWAN

ANDRÉ J. VAN DER WESTHUYSEN, MARCEL ZIJLEMA*
AND JURJEN A. BATTJES

Faculty of Civil Engineering and Geosciences,
Delft University of Technology,
Stevinweg 1, 2628 CN, Delft, The Netherlands
E-mail: a.j.vander.westhuysen@citg.tudelft.nl

**Also: National Institute for Coastal and Marine Management/RIKZ,*
Kortenaerkade 1, 2500 EX, The Hague, The Netherlands

Two aspects that affect the accuracy of the wave model SWAN, namely the criteria for run termination and the modelling of nonlinear four-wave interactions, are investigated. It is shown that the current criteria for the breaking off of simulations are inadequate. It is demonstrated that a new criterion, based on the curvature of the iteration curve of significant wave height, is more effective in obtaining fully-converged model results. An implementation of the Xnl exact method for computing quadruplet interaction is evaluated. It is shown that with this method fetch-limited growth curves and spectra are in better agreement with observations than when the default Discrete Interaction Approximation (DIA) is used.

1. Introduction

SWAN[a] (Booij *et al.*, 1999) is a third-generation spectral wave model that predicts the variance density spectra of wind waves in shallow water by solving the action balance equation for the propagation, generation and dissipation of waves. Since its initial public release, the model has undergone steady improvement in terms of functionality, modelling and accuracy. However, despite this ongoing development, the model still predicts wave spectra with insufficient accuracy in some cases. Examples of its unsatisfactory performance in coastal regions and inland waters of The Netherlands are given by Jacobse *et al.* (2002) and Bottema *et al.* (2003). These and other studies revealed that SWAN models total wave energy well, but tends

[a]Available at http://www.fluidmechanics.tudelft.nl/swan/index.htm

to underestimate period measures.

To address this issue, a long-term study is being undertaken with the aim of improving overall model accuracy. Causes of unsatisfactory model performance may possibly be found in the basic formulation of the action balance equation, its various source terms and its numerical implementation. Here we will focus on the influence of numerical implementation and the source terms that are active in deep water. The latter are of relevance to coastal application because they shape the spectrum arriving in coastal waters and remain important in the shallow-water source term balance.

A number of issues involved in the numerical implementation of SWAN could negatively affect model accuracy. The present study addresses the criteria for the identification of the point of model convergence. These are shown to have a significant impact on model accuracy. It will be demonstrated that the current default criteria of SWAN can lead to errors in wave height and period results in cases of active wind-wave growth. As remedy, a new, additional convergence criterion, based on the curvature of the iteration curve of significant wave height, is presented and evaluated for stationary simulation. It is found to be more effective in locating the point of model convergence, yielding results that are closer to the fully-converged numerical solution.

The source terms active in deep water are wind input, whitecapping and nonlinear quadruplet interaction. A number of deficiencies in the default formulations, based on Komen *et al.* (1984), and their implementation in SWAN are known. The customary first step in improving the balance of these source terms, also adopted here, is to replace the computationally fast, but rather inaccurate, Discrete Interaction Approximation (DIA) source term for quadruplet interaction with a formulation that calculates the complete Boltzmann integral of Hasselmann (1962). A number of approaches are available for the exact integration of the Boltzmann integral. In this study we have used the Xnl method (Van Vledder and Bottema, 2003), as it is more computationally efficient than the recently-implemented FD-RIAM method (Hashimoto *et al.*, 2003). It will be shown that the exact calculation of quadruplet interaction improves wave spectra and integral parameters (including wave period) of deep-water fetch-limited growth. Due to the high computational cost of using an exact quadruplet source term, the model variant investigated here is considered a research version, not yet intended for operational use.

The structure of this paper is as follows: Section 2 gives a brief description of SWAN. Section 3 presents and evaluates a new curvature-based convergence criterion. Section 4 compares simulation results obtained using the DIA and Xnl source terms for quadruplet interaction. Section 5 closes with a discussion.

2. Model description

In stationary simulations, SWAN computes the evolution of the action density N using the time-independent action balance equation

$$\frac{\partial}{\partial x}(c_{g,x}N) + \frac{\partial}{\partial y}(c_{g,y}N) + \frac{\partial}{\partial \theta}(c_\theta N) + \frac{\partial}{\partial \sigma}(c_\sigma N) = \frac{S_{tot}}{\sigma} \ . \qquad (1)$$

The first two terms on the left-hand side represents the propagation of wave energy in two-dimensional geographical space, where $c_{g,x}$ and $c_{g,y}$ are the wave group velocities, including ambient current. The third term describes depth- and current-induced refraction and the fourth term represents the effect of shifting of the radian frequency (σ) due to variations in depth and mean current. The right-hand side contains the total source term S_{tot} which represents all known physical processes that generate, dissipate or redistribute wave energy:

$$S_{tot} = S_{in} + S_{wc} + S_{nl4} + S_{bot} + S_{nl3} + S_{brk} \ . \qquad (2)$$

We distinguish between source terms that are active primarily in deep water, namely energy transfer from wind to waves (S_{in}), dissipation due to whitecapping (S_{wc}) and nonlinear four-wave interactions (S_{nl4}), and source terms that are active exclusively in shallow water, namely bottom friction (S_{bot}), nonlinear three-wave interactions (S_{nl3}) and depth-induced breaking (S_{brk}). Equation (1) is numerically implemented with an implicit four-sweep scheme for propagation in geographical space and a hybrid upwind-central scheme in frequency- and directional spaces (Booij *et al.*, 1999 and Zijlema and Van der Westhuysen, 2004).

3. Convergence criteria

3.1. *Method*

Due to refraction and nonlinear wave energy transfer, interactions occur between the directional quadrants of the four-sweep geographical propagation scheme. To properly take these interactions into account, the quadrant sweeping and the solution of Eq. (1) need to be repeated until some convergence criteria are met. Currently, simulations are terminated when

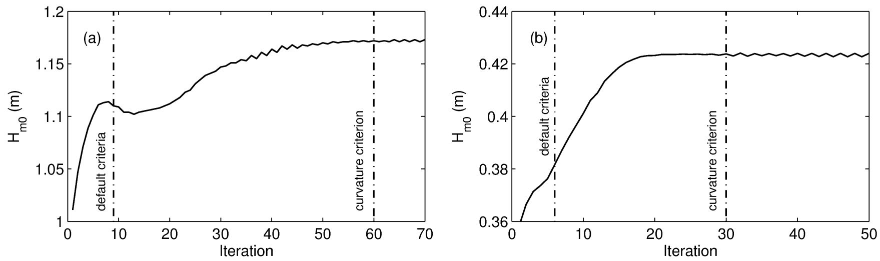

Figure 1. Iteration behaviour of H_{m0} at a single grid point for test cases of (a) Haringvliet Estuary, The Netherlands and (b) Lake George, Australia. Also shown are the locations of run termination using the default convergence criteria (3) and (4) (with $\varepsilon^{\mathrm{r}}_{\mathrm{H}} = \varepsilon^{\mathrm{r}}_{\mathrm{T}} = 0.02$, $\varepsilon^{\mathrm{a}}_{\mathrm{H}} = 0.02$ m and $\varepsilon^{\mathrm{a}}_{\mathrm{T}} = 0.2$ s) and proposed curvature criteria (6) and (3) (with $\varepsilon_{\mathrm{C}} =$ 2e-4, $\varepsilon^{\mathrm{r}}_{\mathrm{H}} = 0.02$ and $\varepsilon^{\mathrm{a}}_{\mathrm{H}} = 0.02$ m).

$$\frac{|\Delta H^s_{m0}(i,j)|}{H^s_{m0}(i,j)} < \varepsilon^{\mathrm{r}}_{\mathrm{H}} \quad \text{or} \quad |\Delta H^s_{m0}(i,j)| < \varepsilon^{\mathrm{a}}_{\mathrm{H}} \tag{3}$$

and

$$\frac{|\Delta T^s_{m01}(i,j)|}{T^s_{m01}(i,j)} < \varepsilon^{\mathrm{r}}_{\mathrm{T}} \quad \text{or} \quad |\Delta T^s_{m01}(i,j)| < \varepsilon^{\mathrm{a}}_{\mathrm{T}} \tag{4}$$

are satisfied in at least 98% of all wet grid points (i,j). Here H^s_{m0} and T^s_{m01} are the significant wave height and mean period at iteration level s, respectively, and $\Delta Q^s \equiv Q^s - Q^{s-1}$, with Q some quantity. The default values of the threshold parameters are $\varepsilon^{\mathrm{r}}_{\mathrm{H}} = \varepsilon^{\mathrm{r}}_{\mathrm{T}} = 0.02$, $\varepsilon^{\mathrm{a}}_{\mathrm{H}} = 0.02$ m and $\varepsilon^{\mathrm{a}}_{\mathrm{T}} = 0.2$ s. Treating the sequence of iteration values as a continuous variable, it can be stated that criteria (3) and (4) check the gradients of the iteration curves of H_{m0} and T_{m01}. This approach would have been sufficient if the convergence of these quantities had been monotonic, as reported by Booij *et al.* (1999). However, inspection of the iteration curves of H_{m0} of typical field case simulations featuring wind-wave growth, taken from Ris *et al.* (2003), shows the contrary (cf. Fig. 1). Iteration curves of SWAN feature characteristic local minima and maxima and small-amplitude oscillations. These occur because of nonlinearities in the source term balance. As a consequence, the default, gradient-based criteria typically terminate iteration at local maxima or minima (Fig. 1a) or local decreases in gradient (Fig. 1b) before convergence is reached.

Considering the non-monotonic nature of the iteration curves, an alternative convergence determinant, namely the second derivative, or curvature, of these curves is proposed. As the solution of a simulation approaches full convergence the curvature of the iteration curves will tend to zero. A robust convergence test will therefore be to terminate iteration when the absolute value of the curvature of these iteration curves falls below a given maximum value. The variable H_{m0} was chosen as convergence measure, since it typically converges slower than T_{m01} and is less sensitive to small oscillations in the spectral tail. What follows can, however, be applied in the same way to T_{m01}. The curvature of the iteration curve of H_{m0} can be expressed in general as

$$\Delta\left(\Delta\tilde{H}^{s}_{m0}\right)^{s} = \tilde{H}^{s}_{m0} - 2\tilde{H}^{s-1}_{m0} + \tilde{H}^{s-2}_{m0}\,, \tag{5}$$

where $\tilde{H}^{s}_{m0}$ is some measure of the significant wave height at iteration level s. To eliminate the effect of small amplitude oscillations on the curvature measure, we define $\tilde{H}^{s}_{m0} \equiv (H^{s}_{m0} + H^{s-1}_{m0})/2$. The resulting curvature-based termination criterion at grid point (i, j) is then

$$\frac{1}{2}|H^{s}_{m0}(i,j) - (H^{s-1}_{m0}(i,j) + H^{s-2}_{m0}(i,j)) + H^{s-3}_{m0}(i,j)|/H^{s}_{m0} < \varepsilon_{\mathrm{C}}\,,\quad s = 3, 4, \ldots\,, \tag{6}$$

where ε_{C} is a given maximum allowable curvature. The curvature measure is made non-dimensional through normalization with H^{s}_{m0}. This curvature requirement is considered to be the primary criterion. However, the curvature passes through zero between local maxima and minima and, at convergence, the solution can oscillate between two constant levels due to the action limiter, while the averaged curvature is zero (cf. Fig. 1). These oscillations may sometimes become excessive. It is therefore proposed to retain, as secondary criterion, the relative and absolute change measures (3). Criteria (6) and (3), the proposed new convergence test, must be satisfied in at least 98% of all wet grid points before the iterative process is terminated. In application, criterion (6) is found to be typically dominant.

3.2. *Results*

Figure 2 presents the behaviour of $|\Delta H^{s}_{m0}|/H^{s}_{m0}$ in criterion (3) and the absolute value of the normalized, average curvature (6) at one grid point during the Lake George simulation corresponding to Fig. 1b. The gradient measure $|\Delta H^{s}_{m0}|/H^{s}_{m0}$ quickly falls below the threshold value of 2%, so that (3), together with criterion (4), terminate the simulation after 6 iterations

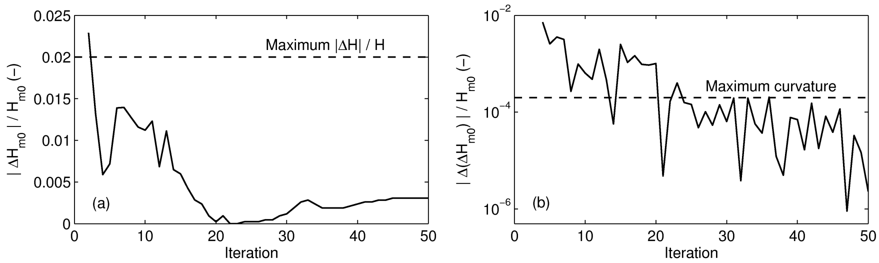

Figure 2. Absolute values of the relative change (panel (a)) and normalized average curvature (panel (b)) at a single grid point for Lake George, plotted against iteration level. The default value of the maximum relative change (2%) and a maximum curvature level of $\varepsilon_{\mathrm{C}} = 2\text{e-}4$ are indicated.

(Fig. 1b). In contrast, the absolute curvature measure, with an appropriate choice of ε_{C}, postpones termination until an iteration level closer to the actual point of convergence. Criteria (6) and (3) are met in 98% of points after 30 iterations (Fig. 1b). Figure 1a presents the corresponding termination point for the Haringvliet simulation. Figure 3 compares the performance of the current default criteria and the new curvature-based criteria with two choices of ε_C for a larger collection of cases from Ris *et al.* (2003). The curvature criteria (6) and (3) yield significant improvement in identifying the point of convergence, with results of H_{m0} and T_{m01} closer to the fully-converged values. By comparing the scatter in the two centre panels, it is also seen that the values of T_{m01} tend converge faster than H_{m0}, supporting the choice of the latter as convergence measure. An obvious result of the application of the new criteria is that the number of run iterations increases, as the underlying iteration behaviour has not been altered. The comparison in Fig. 3 suggests that a value of $\varepsilon_C = 0.001$ for criterion (6) is appropriate for cases in the Dutch coastal region, yielding an average number of iterations between 30 and 50.

4. Nonlinear quadruplet interaction

4.1. *Method*

Nonlinear energy transfer due to resonant third-order wave–wave interactions is described mathematically by the Boltzmann integral for surface gravity waves, proposed by Hasselmann (1962). A set of four waves (a quadruplet) exchanges energy through resonant interaction when the following conditions are met:

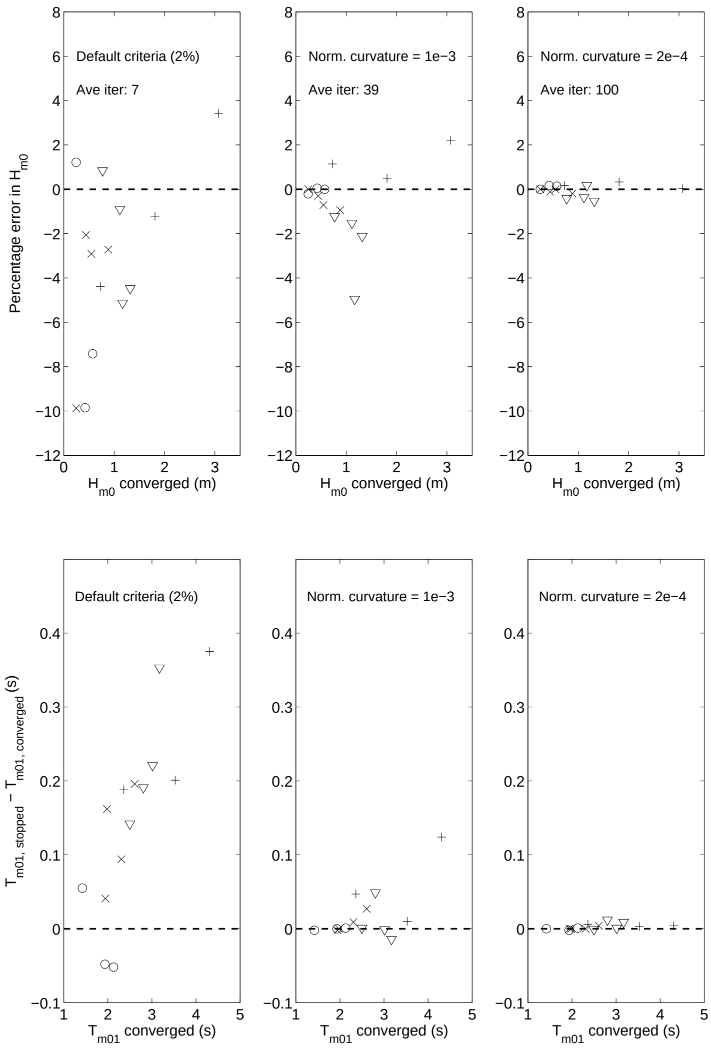

Figure 3. Top panels: Percentage error in H_{m0} at output points incurred using three different stopping criteria, defined as $(H_{m0,stopped} - H_{m0,converged})/H_{m0,converged}$, plotted against $H_{m0,converged}$, for various test cases. Left-hand panel: default criteria, centre panel: new curvature criterion with ε_C = 1e-3, right-hand panel: curvature criterion with ε_C = 2e-4. The average number of iterations before run termination is indicated in each case. Bottom panels: Corresponding results for T_{m01}, expressed in actual error. In all panels the results plotted are of 14 individual cases, featuring: $+$ deep-water fetch-limited growth, $\bigcirc$ Lake George, $\times$ Norderneyer Seegat and $\bigtriangledown$ Haringvliet.

$$\mathbf{k}_1 + \mathbf{k}_2 = \mathbf{k}_3 + \mathbf{k}_4 \tag{7}$$

$$\sigma_1 + \sigma_2 = \sigma_3 + \sigma_4 \tag{8}$$

where $\mathbf{k}_{1..4}$ are the wavenumbers and $\sigma_{1..4}$ the radian frequencies of the four interacting waves, which are in turn related by the linear dispersion relation $\sigma^2 = gk\tanh(kh)$, at a given water depth h. The rate of change of action density at a wavenumber $\mathbf{k}_1$ due to all quadruplet interactions involving $\mathbf{k}_1$ is given by Hasselmann (1962) as

$$\begin{aligned} S_{nl4}(\mathbf{k}_1) = & \iiint G(\mathbf{k}_1, \mathbf{k}_2, \mathbf{k}_3, \mathbf{k}_4)\delta(\mathbf{k}_1 + \mathbf{k}_2 - \mathbf{k}_3 - \mathbf{k}_4)\delta(\sigma_1 + \sigma_2 - \sigma_3 - \sigma_4) \\ & \times [N_1 N_2 (N_3 + N_4) - (N_1 + N_2) N_3 N_4] \, d\mathbf{k}_2 \, d\mathbf{k}_3 \, d\mathbf{k}_4 \end{aligned} \tag{9}$$

in which $N_i = N(\mathbf{k}_i)$ is the action density at the wavenumber $\mathbf{k}_i$, G is a coupling coefficient and δ is the Dirac delta function.

Various numerical integration algorithms for the Boltzmann integral (9) exist. These can be divided into methods aiming at efficiently solving the complete integral (so-called exact methods) and methods that approximate or parameterize the integral in some way, for the sake of computational efficiency. In this study we applied the exact method developed by Webb (1978), Tracy and Resio (1982) and Resio *et al.* (2001). This algorithm was reprogrammed by Van Vledder (Van Vledder and Bottema, 2003, Van Vledder, 2003), bearing the name Xnl.

The most widely-used approximation of Eq. (9) is the Discrete Interaction Approximation (DIA) (Hasselmann *et al.*, 1985), in which only a single interaction quadruplet and its mirror image are used to estimate the energy transfer. The nonlinear transfer computed with the DIA yields a rather inaccurate version of the complete solution of Eq. (9). Analyses of the deficiencies of DIA results by Hasselmann *et al.* (1985) and Van Vledder *et al.* (2000) show, in particular, an incorrect position and width (in frequency space) of its low-frequency positive lobe and an overestimation of its directional width. Therefore, in this study we investigate the changes in simulation results of SWAN when this DIA expression, which is currently used together with the wind input and whitecapping terms of Komen *et al.* (1984), is replaced by the Xnl exact method. It is emphasised that this is merely a first step in an overall improvement of the deep-water source term balance in SWAN, because other source terms also require modification. Moreover, the use of Xnl in an operational model version is very expensive (requiring a factor 300 more computational time).

4.2. *Results*

Figure 4 compares the deep-water, fetch-limited growth curves produced by, respectively, the DIA and Xnl in combination with the default wind input and whitecapping source terms of Komen *et al.* (1984). No recalibration was done for the Xnl case. It is seen that both the DIA and Xnl adequately reproduce the dimensionless energy levels of Kahma and Calkoen (1992) (composite dataset) and Pierson and Moskowitz (1964). In the Kahma and Calkoen range, the simulation with Xnl yields a somewhat better agreement with the dimensionless peak frequency observations than the DIA. The peak periods produced with Xnl in this range are on average 0.2 s higher than those produced with the DIA.

Focussing on the Kahma and Calkoen (1992) fetch range, Fig. 5 shows a comparison between the directionally-integrated frequency spectra produced by the DIA and Xnl and the parametric spectral form of Donelan *et al.* (1985), using the peak frequency of Kahma and Calkoen (1992). The DIA produces a slight overestimation of the peak frequency (as was seen in Fig. 4) and a somewhat broader distribution around the peak. These two characteristics are better reproduced by Xnl. It is noted that, without re-calibration, the energy levels produced by the Xnl simulation are slightly higher than the observed values. Figure 6 shows that Xnl produces significantly narrower directional distributions than the DIA. Also, the distributions produced by Xnl become bi-modal at high wavenumbers relative to the peak, as observed in the field by Hwang *et al.* (2000), whereas those produced by the DIA remain unimodal. A similar transition to bimodality was found in numerical simulations with the WAM model (WAMDI, 1988) when using exact quadruplet interactions (e.g. Banner and Young, 1994).

5. Discussion

In this study aspects of the numerical implementation and deep-water physics of SWAN were considered in an ongoing project to improve the model's overall accuracy. The first subject considered was the criteria for the termination of the iterative solution procedure. It was found that the current default criteria can terminate iteration well before full convergence is reached, leading to potential errors in model results. The addition of a new criterion, based on the curvature of the iteration curve of the significant wave height, was shown to yield results in good agreement with fully-converged values. Since the iteration behaviour of the model was not addressed in this study, this result implies that more iterations are required.

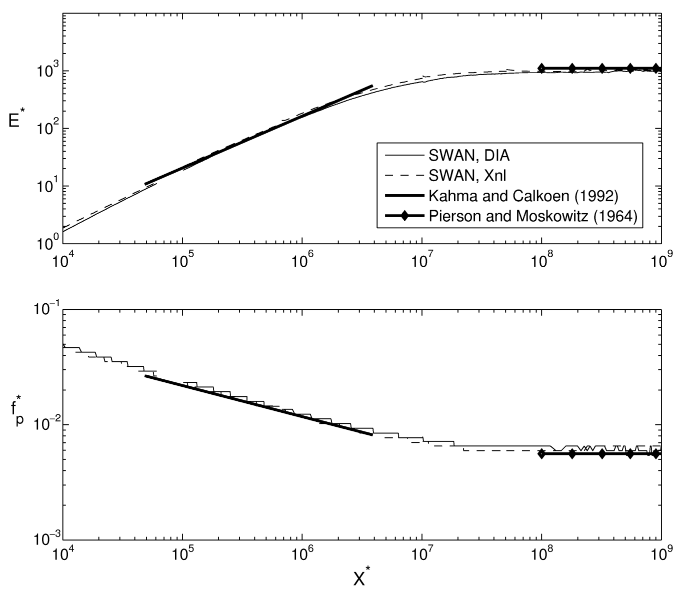

Figure 4. Deep-water, fetch-limited growth curves produced using the DIA and Xnl quadruplet interaction source terms and default Komen *et al.* (1984) formulations for wind and whitecapping. Results for $U_{10} = 10$ m/s, presented in terms of dimensionless energy $E^* = g^2 E_{tot}/u_*^4$ and peak frequency $f_p^* = f_p u_*/g$ as functions of dimensionless fetch $X^* = gX/u_*^2$.

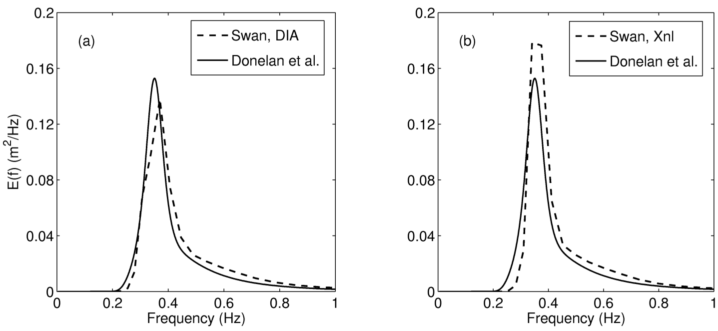

Figure 5. Comparison between the deep-water, fetch-limited spectra produced using the DIA (panel (a)) and the Xnl exact method (panel (b)) and the parametric form of Donelan *et al.* (1985). Peak frequency according to Kahma and Calkoen (1992). Results for $U_{10} = 10$ m/s at $X^* = 6 \times 10^5$.

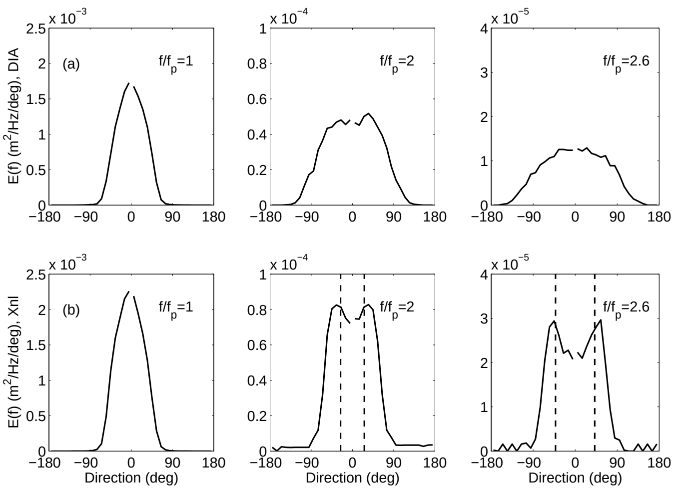

Figure 6. Simulated directional distributions at the peak and energy-containing tail produced using the DIA (row (a)) and the Xnl method (row (b)) at three different frequencies. Results for deep-water, fetch-limited growth with $U_{10} = 10$ m/s at $X^* = 6 \times 10^5$. The dashed lines in row (b) are the locations of the bi-modal peaks observed by Hwang *et al.* (2000).

The number of required iterations may, in turn, be reduced in a number of ways. Firstly, the so-called first guess (Booij et al. 1999), which is used to speed up convergence, can be improved. The smaller the mismatch between the first guess and the converged solution, the fewer iterations are required to reach convergence. A second source of slow convergence is the sometimes erratic iteration behaviour of SWAN, which may be remedied by applying under-relaxation (Zijlema and Van der Westhuysen, 2004).

The second subject of this paper was the evaluation of the Xnl exact method for calculating quadruplet interactions. It was shown that SWAN with Xnl reproduces deep-water, fetch-limited growth curves well, yielding a somewhat higher peak period than with the DIA. The exact method yields frequency- and directional distributions that are in better agreement with observations than those produced using the DIA. In particular, the Xnl method yields bi-modal directional distributions over the frequency range $f/f_p \geq 2$. These improvements, however, come at increased computational cost. Work is under way by a number of researchers to retain the key results of exact quadruplet algorithms, whilst improving computational speed (e.g. Hashimoto *et al.*, 2003 and Van Vledder *et al.*, 2000).

Acknowledgments

We are grateful to G. van Vledder for providing us with the Xnl code and for his assistance in its implementation in SWAN. This study is supported by the National Institute for Coastal and Marine Management/RIKZ of the Ministry of Transport, Public Works and Water Management through the project RKZ-1124.

References

Banner, M. L. and I. R. Young. 1994. Modelling spectral dissipation in the evolution of wind waves. Part I: Assessment of existing model performance, J. of Phys. Oceanogr., 24(7), 1550–1571.

Booij, N., R. C. Ris and L. H. Holthuijsen. 1999. A third-generation wave model for coastal regions, Part I, Model description and validation, J. of Geophys. Res., 104 (C4), 7649–7666.

Bottema, M., J. P. De Waal and E. J. Regeling. 2003. Some applications of the Lake IJssel/Lake Sloten wave data set. Proc. 28th Int. Conf. on Coastal Eng., ASCE, 413–425.

Donelan, M. A., J. Hamilton and W. H. Hui. 1985. Directional spectra of wind-generated waves, Phil. Trans. Roy. Soc. London, A315, 509–562.

Hashimoto, N., IJ. G. Haagsma and L. H. Holthuijsen. 2003. Four-wave interactions in SWAN, Proc. 28th Int. Conf. Coastal Eng., ASCE, 392–404.

Hasselmann, K. 1962. On the non-linear energy transfer in a gravity-wave spectrum. Part 1. General theory, J. Fluid Mech., 12(4), 481–500.

Hasselmann, S., K. Hasselmann, J. A. Allender and T. P. Barnett. 1985. Computations and parameterizations of the nonlinear energy transfer in a gravity wave spectrum. Part 2: Parameterization of the nonlinear transfer for application in wave models, J. of Phys. Oceanogr., 15, 1378–1391.

Hwang, P. A., D. W. Wang, E. J. Walsh, W. B. Krabill and R. N. Shift. 2000. Airborne measurements of the wavenumber spectra of ocean surface waves. Part 2. Directional distribution, J. of Phys. Oceanogr., 30, 2768–2787.

Jacobse, J. J., A. T. M. M. Kieftenburg and F. Den Heijer. 2002. Reliability of wave conditions calculated with SWAN (in Dutch), Report No. RIKZ/OS-2002.116x, Rijksinstituut voor Kust en Zee/RIKZ, 40 pp.

Kahma, K. K. and C. J. Calkoen. 1992. Reconciling discrepancies in the observed growth of wind-generated waves, J. of Phys. Oceanogr., 22, 1389–1405.

Komen, G. J., S. Hasselmann and K. Hasselmann. 1984. On the existence of a fully developed wind-sea spectrum, J. of Phys. Oceanogr., 14, 1271–1285.

Pierson, W. J. and L. Moskowitz. 1964. A proposed spectral form for fully developed wind seas based on the similarity theory of S. A. Kitaigorodskii, J. Geophys. Res., Vol. 69, 5181–5190.

Resio, D. T., J. H. Pihl, B. A. Tracy and C. L. Vincent. 2001. Nonlinear energy fluxes and the finite depth equilibrium range in wave spectra, J. Geophys. Res., Vol. 106, No. C4, 6985–7000.

Ris, R. C., L. H. Holthuijsen, J. M. Smith, N. Booij and A. van Dongeren. 2003.

The ONR Test Bed for coastal and oceanic wave models, Proc. 28th Int. Conf. Coastal Eng., ASCE, 380–391.

Tracy, B. A. and D. T. Resio. 1982. Theory and calculation of the nonlinear energy transfer between sea waves in deep water, WIS Rep. 11, U.S. Army Engineer Waterways Experiment Station, 48 pp.

Van Vledder, G. Ph. 2003. Computational methods for the calculation of non-linear quadruplet wave–wave interactions, Report A951, Alkyon Hydraulic Consultancy and Research, 52 pp.

Van Vledder, G. Ph. and M. Bottema. 2003. Improved modelling of nonlinear four-wave interactions in shallow water, Proc. 28th Int. Conf. Coastal Eng., ASCE, 459–471.

Van Vledder, G. Ph., T. H. C. Herbers, R. J. Jensen, D. T. Resio and B. A. Tracy. 2000. Modelling of non-linear quadruplet wave–wave interactions in operational wave models, Proc. 27th Int. Conf. Coastal Eng., ASCE, 797–811.

WAMDI group. 1988. The WAM model - a third generation ocean wave prediction model, J. Phys. Oceanogr., 18, 1775–1810.

Webb, D. J. 1978. Non-linear transfers between sea waves, Deep-Sea Res., 25(3), 279–298.

Zijlema, M. and A. J. van der Westhuysen. 2004. On convergence behaviour and numerical accuracy in stationary SWAN simulations of nearshore wind wave spectra, *Submitted to Coastal Engineering*.

KEYWORDS - ICCE 2004

IMPROVEMENT OF THE NUMERICS AND DEEP-WATER PHYSICS IN AN ACADEMIC VERSION OF SWAN
A. J. van der Westhuysen, M. Zijlema and J. A. Battjes
Abstract No. 8

Spectral wave modelling
Numerics
Stationary simulation
Convergence criteria
Nonlinear quadruplet interaction